

Uncertainty Quantification for Deep Learning

Peter Jan van Leeuwen^{1,2}, J. Christine Chiu¹, and C. Kevin Yang¹

¹Department of Atmospheric Science, Colorado State University, Fort Collins, CO, USA,

²Department of Meteorology, University of Reading, Reading, UK,

Correspondence to: **Peter Jan van Leeuwen** (peter.vanleeuwen@colostate.edu)

Abstract. A complete and statistically consistent uncertainty quantification for deep learning is provided, including the sources of uncertainty arising from (1) the new input data, (2) the training and testing data (3) the weight vectors of the neural network, and (4) the neural network because it is not a perfect predictor. Using Bayes Theorem and conditional probability densities, we demonstrate how each uncertainty source can be systematically quantified. We also introduce a fast and practical way to incorporate and combine all sources of errors for the first time. For illustration, the new method is applied to quantify errors in cloud autoconversion rates, predicted from an artificial neural network that was trained by aircraft cloud probe measurements in the Azores and the stochastic collection equation formulated as a two-moment bin model. For this specific example, the output uncertainty arising from uncertainty in the training and testing data is dominant, followed by uncertainty in the input data, in the trained neural network, and uncertainty in the weights. We discuss the usefulness of the methodology for machine learning practice, and how, through inclusion of uncertainty in the training data, the new methodology is less sensitive to input data that falls outside of the training data set.

1. Introduction

Many processes in geosciences are highly complex and computationally challenging, or even not well known. For those processes, machine learning, and especially deep learning, becomes widely used to either replace expensive numerical schemes and models or to describe relations between variables where the underlying equations are unknown. For example, radiative transfer is known but expensive to compute, while cloud microphysical processes are known to a large extent, but not at the scales used for weather or climate prediction. Despite successful applications in such processes, the uptake of deep learning in science has been slow, mainly because proper uncertainty estimates are lacking and yet critical for comparison studies, forecasting, and risk management.

Deep Learning can be considered as a method that provides a map between an input vector x and an output vector z :

$$z = f(x, w) \tag{1}$$

where $f(x, w)$ denotes the neural network (NN), which is a function of an input vector x and a weight vector w . The weight vector w is determined via an estimation process based on the training dataset that contains many input-output pairs of data. The function f is special in that it comprises a hierarchy of nonlinear scalar functions within other scalar functions. The NN is extremely flexible and can fit almost any training data because of the large size of the weight vector (e.g., order 5000 or more). To simplify the discussion, this weight vector w in Eq. (1) includes both the so-called weights and the biases from the machine learning literature.

Several sources contribute to the uncertainty in the output z . From Eq. (1), we see clear contributions from the uncertainty in the input vector x , uncertainty in the weight vector w , and uncertainty in the functional form of $f(\cdot)$ because the NN will not be perfect in mapping input to the output vector. Because w is trained and evaluated using training and testing data, uncertainties in these data should also be considered, although they are not explicitly shown in Eq. (1). The other uncertainty source that is not shown in Eq. (1) arises when the new input vector x falls outside the range of the training and testing datasets.

Since in that case there is no principled approach to take that uncertainty into account (see Discussions section), we will focus on the first four sources of uncertainty in this study. Once all four sources of uncertainties are quantified, they should be combined to form the total uncertainty in z , which will be described by a probability density function (pdf). However, up to now, there is no practical method that incorporates all uncertainty sources into this pdf.

To better explain the underlying difficulty and the incompleteness of existing methods for uncertainty quantification, we need to refer to Bayes Theorem. This theorem states that the pdf of a random variable A given knowledge of a variable B , $p(A|B)$, can be expressed as the pdf of random variable A without knowing B , so $p(A)$, and the likelihood $l(B|A)$, as:

$$p(A|B) = \frac{l(B|A)p(A)}{p(B)} \quad (2a)$$

We call $p(A)$ the prior pdf of A , and $p(A|B)$ the posterior pdf of A . The pdf of B in the denominator is a normalization factor because B is not a random variable, but has a given value. $l(B|A)$ represents the likelihood that A gives rise to B , which is a function of random variable A . It determines how likely it is to find value B for each value of random variable A . For future reference, we also use the theorem in the form of

$$p(A|B, C) = \frac{l(B|A, C)p(A|C)}{p(B|C)} \quad (2b)$$

which is just Bayes Theorem with all the terms conditioned on another set of variables C .

Among the main sources of uncertainty mentioned above, most attention has been given to the uncertainty in the weight vector w and the uncertainty in the trained neural network f . In theory, the uncertainty of w in an NN can be derived directly from Bayes Theorem, which is the basis of Bayesian Deep Learning (e.g., MacKay, 1992; Neal, 1995; Andrieu et al., 2003). From Eq. (2a), if we choose $A = w$ and $B =$ training data, we know that the posterior uncertainty in w given a training dataset is determined by the prior uncertainty in w , and a likelihood that indicates how likely the training data are if the weight vector is equal to a certain w . Since the function f in deep learning is highly nonlinear, this likelihood, and hence the uncertainty pdf for the weight vector w , will have an extremely complex shape (e.g., many local minimums and maximums). For low-dimensional systems, one can use methods such as Markov-Chain Monte Carlo (MCMC), Langevin sampling, and Hybrid or Hamiltonian MC to accurately describe the posterior pdf (e.g., Doucet et al., 2003, Van Leeuwen, 2015), but these methods do not scale well for high-dimensional problems, which are often the case in deep learning applications. To alleviate this issue, approximations to the posterior pdf have been proposed, such as the Gaussian approximation, or variational Bayes (approximated pdf by a finite set of pdfs of a certain shape, e.g., a Gaussian mixture). Apart from the crude Gaussian approximation, all these methods remain very expensive in high-dimensional problems, which pose difficulties in practice (e.g., Blundell et al., 2015).

A popular machine-learning method for uncertainty quantification related to the weights w is Bootstrapping or *Bagging* (Breiman, 1996), which uses an ensemble of weight vectors to generate an ensemble of outputs. In this method, the weight vector ensemble can be generated in several ways, e.g., by randomly drawing initial weights and by randomly varying the order in which training batches are used during training of the NN, or by giving each NN a subset of the training data. Each *trained* weight vector in the resulting ensemble is used to generate one output value and interpreted to have the same probability. This, then, results in an ensemble of output values that is suggested to represent its uncertainty pdf. Unfortunately, while this method gives a spread in the output values, this spread does not represent a proper uncertainty estimate. The reason is that during training, the ensemble of initial weight vectors is transformed into an ensemble of trained weight vectors. Because of the nonlinear transformation during the training process, the pdf of the equally probable *initial* weight vectors is deformed into a pdf with a complicated shape determined by the likelihood of each weight vector to produce the training data (corresponding to the $l(B|A)$ factor above). Hence, the *trained* weight vectors are in fact, not equally likely anymore, and so are the output values. A simple treatment of equally likely output values as assumed in Bagging is inappropriate.

This issue with the likelihood of the weight vectors is more troublesome than anticipated. In theory, the likelihood value of each trained weight vector, also called importance weight, can be properly calculated and included to evaluate the ensemble of weight vectors. However, in practice, we would find that one particular weight vector provides a better fit to the training data than all the other members, and hence has a much larger importance weight than the others. As a result, the overwhelming importance of one member and the negligible influence of others essentially lead to an ensemble of one weight vector, which, consequently, would have zero uncertainty. This issue is well recognized in Bayesian Deep Learning in which efforts have been made to ensure an equally likely ensemble of trained weight vectors, but this problem is ignored in Bagging. We will elaborate on this delicate point in section 3.3.

Another popular method for uncertainty quantification related to the weights w is *Monte-Carlo Dropout* (Gal & Ghahramani, 2016). In conventional dropout, a method used to avoid overfitting, the weight of each neuron is set to zero during the training phase with a probability p . After training, all weights are used but their trained value is multiplied by p to generate one NN. In Monte-Carlo Dropout, the same dropout procedure used during training is also used during prediction. In other words, the trained weights are also put randomly to zero with probability p during prediction. This prediction procedure is performed several times to generate an ensemble of weight vectors, leading to an ensemble of output values. This output ensemble is then suggested to provide an uncertainty estimate. The issue with this method is that during training one realization of a trained weight vector is created. Then this weight vector is randomly perturbed by dropout to generate an ensemble of perturbed trained weight vectors. What should be the next step is to weigh each of those perturbed weight vectors by their likelihood value, as discussed above for Bagging, but that step is omitted. Hence, similar to Bagging, the uncertainty quantification is inappropriate. In addition, there are other issues with this method, related to the fact that the posterior uncertainty does not decrease when more data is used, as a proper uncertainty estimate should do (see e.g., Osband, 2016, Verdoja and Kyrki, 2021, and references in these papers).

A second category of approaches tries to estimate the pdf of output uncertainty directly. Instead of predicting output z , the NN predicts:

$$p_z = f_p(x, w_p) \quad (3)$$

where p_z denotes the uncertainty pdf of output z , and the subscript p on the weight vector w and on f denotes that the target of estimation is p_z , not z itself as in Eq (1). The difference from the methods above is that the uncertainty pdf in z is not determined via an ensemble of weight vectors w , but instead one weight vector is trained to provide the pdf directly. The pdf p_z can be characterized in two ways. It can be described by parameters, such as mean and variance (e.g., Nix and Weigend, 1994; Wang et al, 2016) or by its histogram (e.g., Wang et al., 2016; Pfreundschuh et al., 2018; Sonderby et al., 2020). The parameter-based approach requires choosing the shape of the output pdf beforehand, which is a disadvantage compared to the histogram-based method. The histogram-based methods work for a low-dimensional output space and become impractical in high-dimension problems, because the number of output variables required to describe histograms increases dramatically with the dimension.

A third category can be considered as a mixture of the two approaches. It trains an NN that will act as a generator of samples of p_z (e.g. Sohl-Dickstein et al., 2015; Price et al, 2023). The method starts with training data pairs (X_m, Z_m) and adds noise with a known noise distribution to the outputs Z_m . This results in a set of noisy output samples Z_m^{noise} . Then the method trains a so-called denoiser to recover the original output training data Z_m from these noisy output values, conditioned on the original inputs X_m . It then takes the noisy output samples Z_m^{noise} and adds another noise term to each of them. And again, a denoiser is trained, this time to get the Z_m^{noise} samples back. In this way a sequence of denoisers is trained, one for each time noise is added. Each of these denoisers is conditioned on X_m , or, in other words, there is a different set of denoisers for each X_m . Finally, after noise is added several times, the output data loses all structure and is essentially pure noise. This means that if we now start from a pure noise sample, and push it backward through all denoisers, we obtain a sample from the distribution of the training data. Hence, to obtain an output sample to a new input x , we use the denoisers *conditioned on x* to generate the output sample starting from a pure noise sample. By generating several pure noise samples and push each of them through the

denoisers *conditioned on* x , we obtain a set of output samples that describe the uncertainty pdf p_z . This method is very efficient even in high-dimensional spaces.

The methods in the second and third categories, however, ignore the uncertainty in the weight vector w_p . This omission is partly corrected in so-called Deep Ensembles (Lakshminarayanan et al., 2017). Deep Ensembles generates an ensemble of pdf parameters, or an ensemble of histograms using an ensemble of initial untrained weight vectors and training batch orders. The resulting ensemble of pdf parameters is further averaged to represent the pdf of z , or the histograms themselves are averaged. Similar to Bagging and MC dropout, the simple average of the ensemble overlooks the fact that the trained weight vectors w_p , and thus the output ensemble members, are not equally likely.

As mentioned above, the literature has concentrated on quantifying uncertainty in the weight vector w or tried to estimate the uncertainty pdf of z directly. None of the machine-learning methods discussed above have considered the uncertainty in the training and testing data, or in the new input data. While the uncertainty in the training, testing, and new input data might be small in some fields, it can be a large factor in the geoscience data, e.g., direct measurements, model output, or reanalysis data. Compared to the real world, they all have errors that should not be ignored.

To conclude, many methods have been developed for quantifying uncertainty in the output of a deep-learning NN, but they are either incomplete and/or statistically inappropriate. The recent article by Abdar et al. (2021) gives a comprehensive overview of what has been used, but a critical discussion of the different methodologies is not provided. The review by Cheng et al. (2023) discusses the connection between data assimilation, machine learning, and uncertainty quantification, but the uncertainty quantification methods mentioned above are quoted without a critical review.

In this paper, we will for the first time take all uncertainty sources into account, derive an expression for the exact pdf, and provide an efficient methodology for practical calculations. In Section 2, we describe how to include all uncertainty sources systematically. In Section 3, we introduce a practical way to calculate the relevant uncertainty sources and put them all together. Specifically, we will explain how we use so-called proposal densities, a standard method in statistics, to resolve the likelihood issue of the trained weight vectors w . In Section 4, we demonstrate an application for predicting cloud process rates from an NN and provide a physical interpretation of the resulting uncertainty. Finally, conclusions and discussions are provided in the last section.

2. Uncertainty propagation in Deep Learning

The uncertainty in the output z can be described by the pdf $p(z|x, \theta_{tr}, \theta_{te})$, which is the pdf of z given an input vector x and training and testing data θ_{tr} and θ_{te} . The training and testing data consist of input and output pairs (X, Z) . The first step in deriving $p(z|x, \theta_{tr}, \theta_{te})$ is to incorporate the uncertainty in the input vector x . Following ideas from data assimilation (e.g., Van Leeuwen, 2015; 2020, and Evensen et al., 2022), we can consider x as a random draw from a distribution $p(x)$, centered around a true input vector. This true input vector is not known, but, as we will show later, this is not a concern. Let us consider all possible true input vectors that would lead to us drawing x . We denote these possible true inputs by x^t . We now use the identity:

$$p(A|C) = \int p(A, B|C) dB \quad (4)$$

to incorporate the uncertainty in the new input vector x as follows:

$$p(z|x, \theta_{tr}, \theta_{te}) = \int p(z, x^t|x, \theta_{tr}, \theta_{te}) dx^t$$

$$= \int p(z|x^t, x, \theta_{tr}, \theta_{te}) p(x^t|x, \theta_{tr}, \theta_{te}) dx^t = \int p(z|x^t, \theta_{tr}, \theta_{te}) p(x^t|x) dx^t, \quad (5)$$

where for the second equality, the identity

$$p(A, B|C) = p(A|B, C)p(B|C) \quad (6)$$

is used. For the third equality, we used that, if the true input was x^t , then x does not provide extra information on z . Furthermore, since input vectors do not depend on the training or testing data, we have $p(x^t|x, \theta_{tr}, \theta_{te}) = p(x^t|x)$. This pdf describes the probability of each possible true input x^t given that we have input sample x . This pdf is exactly the uncertainty pdf of x , as that uncertainty pdf describes the probability of the true input by definition.

The second step is to incorporate the uncertainty in the training and testing data. We can consider the training and testing data pairs as a random draw from a distribution $p(\theta_{tr}, \theta_{te})$, centered around the true data $(\theta_{tr}^t, \theta_{te}^t)$, where the subscript tr and te denote the data from the training and testing set, respectively. Similar to the way of how the new input vector x is handled, let us consider all possible true training and testing data $(\theta_{tr}^t, \theta_{te}^t)$ that would lead us to draw $(\theta_{tr}, \theta_{te})$. This allows us to write:

$$\begin{aligned} p(z|x, \theta_{tr}, \theta_{te}) &= \int p(z|x^t, \theta_{tr}, \theta_{te}) p(x^t|x) dx^t \\ &= \iiint p(z, \theta_{tr}^t, \theta_{te}^t | x^t, \theta_{tr}, \theta_{te}) p(x^t|x) d\theta_{tr}^t d\theta_{te}^t dx^t \\ &= \iiint p(z|x^t, \theta_{tr}^t, \theta_{te}^t) p(\theta_{tr}^t|\theta_{tr}) p(\theta_{te}^t|\theta_{te}) p(x^t|x) d\theta_{tr}^t d\theta_{te}^t dx^t, \end{aligned} \quad (7)$$

where we used the identity in Eq. (6) and the same reasoning as for the new input x . We also used that the uncertainties in training and testing data are independent.

We now incorporate the uncertainty of weight vector that defines the neural network. We can write

$$\begin{aligned} p(z|x, \theta_{tr}, \theta_{te}) &= \iiint p(z|x^t, \theta_{tr}^t, \theta_{te}^t) p(\theta_{tr}^t|\theta_{tr}) p(\theta_{te}^t|\theta_{te}) p(x^t|x) d\theta_{tr}^t d\theta_{te}^t dx^t \\ &= \iiint p(z, w|x^t, \theta_{tr}^t, \theta_{te}^t) p(\theta_{tr}^t|\theta_{tr}) p(\theta_{te}^t|\theta_{te}) p(x^t|x) d\theta_{tr}^t d\theta_{te}^t dw dx^t, \end{aligned} \quad (8)$$

We now evaluate further

$$p(z, w|x^t, \theta_{tr}^t, \theta_{te}^t) = p(z|w, x^t, \theta_{tr}^t, \theta_{te}^t) p(w|x^t, \theta_{tr}^t, \theta_{te}^t) = p(z|w, x^t, \theta_{te}^t) p(w|\theta_{tr}^t) \quad (9)$$

where we used that if the weight vector is given, the training data do not provide extra information on z . Furthermore, the weight vector w by definition is only dependent on the training data and does not depend on the testing data and x^t .

Putting Eq. (9) in Eq. (8), we find:

$$p(z|x, \theta_{tr}, \theta_{te}) = \iiint p(z|w, x^t, \theta_{te}^t) p(w|\theta_{tr}^t) p(\theta_{tr}^t|\theta_{tr}) p(\theta_{te}^t|\theta_{te}) p(x^t|x) d\theta_{tr}^t d\theta_{te}^t dw dx^t. \quad (10)$$

The right-hand side of Eq. (10) highlights the sources of the uncertainty in z , namely (1) uncertainty in the new input, via $p(x^t|x)$, (2) uncertainty in the data pairs in the training and testing sets via $p(\theta_{tr}^t|\theta_{tr})$ and $p(\theta_{te}^t|\theta_{te})$, (3) uncertainty in the weights via $p(w|\theta_{tr}^t)$, and (4) the uncertainty in the NN because the NN is not a perfect predictor, via $p(z|w, x^t, \theta_{te}^t)$. These four pdfs will be estimated and discussed individually in the following section.

3. A practical method for uncertainty quantification

3.1 Source 1: Uncertainty in x

The influence of uncertainty in the input vector x on the output z is the easiest to implement. A number of N_x samples can be drawn from the uncertainty pdf of the input vector x , centred on that input vector, and then pushed through the NN to generate samples of the output. Mathematically, this means that we draw the samples from the uncertainty pdf, $p(x^t|x)$, as:

$$p(x^t|x) = \frac{1}{N_x} \sum_{i=1}^{N_x} \delta(x^t - x_i^t) \quad (11)$$

where x_i^t are the drawn samples centered around x . Using this expression, we can rewrite Eq. (10) as:

$$p(z|x, \theta_{tr}, \theta_{te}) = \frac{1}{N_x} \sum_{i=1}^{N_x} \iiint p(z|w, x_i^t, \theta_{te}^t) p(w|\theta_{tr}^t) p(\theta_{tr}^t|\theta_{tr}) p(\theta_{te}^t|\theta_{te}) d\theta_{tr}^t d\theta_{te}^t dw. \quad (12)$$

3.2 Source 2: Uncertainty in the training and testing data

The uncertainty in the training and testing data can be treated in the same way as the uncertainty in the new input vector x . Similar to Eq. (11), we draw samples from $p(\theta_{tr}^t|\theta_{tr})$ and $p(\theta_{te}^t|\theta_{te})$ and write:

$$p(\theta_{tr}^t|\theta_{tr}) = \frac{1}{N_{X1}} \sum_{j1=1}^{N_{X1}} \delta(\theta_{tr}^t - \theta_{tr,j1}^t) \quad (13)$$

and similar for $p(\theta_{te}^t|\theta_{te})$. This leads to:

$$p(z|x, \theta_{tr}, \theta_{te}) = \frac{1}{N_x} \sum_{i=1}^{N_x} \frac{1}{N_{X1}} \sum_{j1=1}^{N_{X1}} \frac{1}{N_{X2}} \sum_{j2=1}^{N_{X2}} \int p(z|w, x_i^t, \theta_{te,j2}^t) p(w|\theta_{tr,j1}^t) dw \quad (14)$$

where N_{X1} and N_{X2} are the number of samples drawn from the uncertainty pdf of the input-output pairs in the training and testing datasets, respectively.

3.3 Source 3: Uncertainty in the weights

3.3.1 Basic derivation

We now determine the pdf of the weights conditioned on training data in Eq. (14), $p(w|\theta_{tr,j1}^t)$. As mentioned in the Introduction, this pdf is complicated due to the complex relation between weights and the training data. Hence, we do not know what this pdf looks like, and we also do not know how to draw samples from it. Instead, we will use elements of the machine-learning practice, as follows. The weights are trained following a certain minimization recipe. Supposing that the NN architecture and the minimization procedure are fixed, the resulting weight vector will then only depend on the initial weight vector and the batch order. By denoting the batch order b , we can write:

$$\begin{aligned} p(w|\theta_{tr,j1}^t) &= \int p(w, b|\theta_{tr,j1}^t) db \\ &= \int p(w|b, \theta_{tr,j1}^t) p(b|\theta_{tr,j1}^t) db = \int p(w|b, \theta_{tr,j1}^t) p(b) db, \end{aligned} \quad (15)$$

where we used the fact that the batch order is independent of the training data. By further employing Bayes Theorem in the form of Eq. (2b), and writing the input-output pair of $\theta_{tr,j1}^t$ as $(X_{tr,j1}^t, Z_{tr,j1}^t)$:

$$p(w|b, X_{tr,j1}^t, Z_{tr,j1}^t) = \frac{l(Z_{tr,j1}^t|w, b, X_{tr,j1}^t)}{p(Z_{tr,j1}^t|b, X_{tr,j1}^t)} p(w|b, X_{tr,j1}^t). \quad (16)$$

Note that $p(w|b, X_{tr,j1}^t) = p(w)$, because without being conditioned by the output component in the training data, the weights cannot be determined, and thus its pdf will be no different from the prior. The likelihood $l(Z_{tr,j1}^t|w, b, X_{tr,j1}^t)$ denotes how likely it is that weight vector w and batch order b transfer the input to the output component of the training dataset. As explained in the Introduction, the denominator, $p(Z_{tr,j1}^t|b, X_{tr,j1}^t)$, is a normalization factor that we do not have to calculate explicitly.

Putting Eq. (16) to Eq. (15), we find:

$$p(w|\theta_{tr,j1}^t) = p(w|X_{tr,j1}^t, Z_{tr,j1}^t) = \int \frac{l(Z_{tr,j1}^t|w, b, X_{tr,j1}^t)}{p(Z_{tr,j1}^t|b, X_{tr,j1}^t)} p(w) p(b) db. \quad (17)$$

In the next section, we focus on determining the likelihood $l(Z_{tr,j1}^t|w, b, X_{tr,j1}^t)$ and show how to perform the integral.

3.3.2 The likelihood and the integral

To determine the likelihood, we use the relation between the training pairs and the weight vectors as specified by the neural network:

$$Z_{tr,j1}^t = f(X_{tr,j1}^t, w, b) + \varepsilon(X_{tr,j1}^t), \quad (18)$$

where $\varepsilon(X_{tr,j1}^t)$ is the difference between the predicted $f(X_{tr,j1}^t, w, b)$ and the output of training $Z_{tr,j1}^t$. Because we already incorporated the uncertainty in the input and output training data above in Section 3.2, we can interpret this difference as the uncertainty in the NN function f .

Taking the common practice in machine learning as an example, the uncertainty in each element of the vector $\varepsilon(X_{tr,j1}^t)$ is independent from any other element of that vector and is described by a Gaussian distribution with a zero mean and an error

variance of σ_f^2 . Since $\varepsilon(X_{tr,j1}^t)$ is equal to the difference $Z_{tr,j1}^t - f(X_{tr,j1}^t, w, s)$, each element of this difference is also Gaussian distributed with mean zero and error variance σ_f^2 . We thus find for the likelihood:

$$l(Z_{tr,j1}^t | w, b, X_{tr,j1}^t) = A \cdot \exp \left[-\frac{1}{2} \sum_{m=1}^{N_{tr}} \frac{(Z_{tr,j1,m}^t - f(X_{tr,j1,m}^t, w, b))^2}{\sigma_f^2} \right], \quad (19)$$

where A is a normalization factor, N_{tr} is the total number of the input-output pairs in the training dataset, and the subscript m represents the m -th element of $Z_{tr,j1}^t$.

To calculate the integral in Eq. (17), we draw initial weight vector samples w_k from $p(w)$ and batch order samples b_k from $p(b)$, which leads to:

$$p(w | X_{tr,j1}^t, Z_{tr,j1}^t) = \frac{1}{N_w} \sum_{k=1}^{N_w} \frac{l(Z_{tr,j1}^t | w_k, b_k, X_{tr,j1}^t)}{p(Z_{tr,j1}^t | b_k, X_{tr,j1}^t)} \delta(w - w_k), \quad (20)$$

where N_w is the total number of drawn weight vector samples.

This expression shows that the posterior pdf of the weight vectors would be represented by the initial weight vectors w_k , each with a so-called importance weight:

$$\alpha_{j1,k} = \frac{1}{N_w} \frac{l(Z_{tr,j1}^t | w_k, b_k, X_{tr,j1}^t)}{p(Z_{tr,j1}^t | b_k, X_{tr,j1}^t)}. \quad (21)$$

This means that if one calculates any posterior moment associated with w (e.g., mean or covariance), that moment should be weighted by importance weights $\alpha_{j1,k}$. However, $\alpha_{j1,k}$ values vary enormously between samples – one of them would have a value close to 1, while all others have values very close to zero. This is because the likelihood contains an exponential term, as shown in Eq. (19). The sum in the brackets varies considerably with the weight vector w_k , and the exponent of that sum will enhance that variation substantially. As a result, only one weight vector is important for describing $p(w | X_{tr,j1}^t, Z_{tr,j1}^t)$; the ensemble reduces effectively to one member, and the uncertainty is reduced to zero. This issue is known as filter degeneracy in the particle filter literature (Doucet et al, 2000; Van Leeuwen et al, 2019; Evensen et al, 2022), and makes Eqs. (20) and (21) not practical.

3.3.3 The proposal density

Unlike Eq. (20) that draws weights from the pdf of the untrained weights for calculating the integral, we could use trained weights instead. Mathematically, this can be accommodated by introducing a so-called proposal density that depends on the training data $q(w | X_{tr,j1}^t, Z_{tr,j1}^t)$ (Doucet et al, 2000, Van Leeuwen, 2010; Ades and Van Leeuwen, 2012). First, we rewrite the integral by multiplying and dividing by proposal density $q(w | X_{tr,j1}^t, Z_{tr,j1}^t)$, and then sample from $q(w | X_{tr,j1}^t, Z_{tr,j1}^t)$ instead of from $p(w)$. This leads to:

$$p(w | X_{tr,j1}^t, Z_{tr,j1}^t) = \int \frac{l(Z_{tr,j1}^t | w, b, X_{tr,j1}^t)}{p(Z_{tr,j1}^t | b, X_{tr,j1}^t)} p(w) p(b) db$$

$$\begin{aligned}
&= \int \frac{l(Z_{tr,j1}^t | w, b, X_{tr,j1}^t)}{p(Z_{tr,j1}^t | b, X_{tr,j1}^t)} \frac{p(w)}{q(w | X_{tr,j1}^t, Z_{tr,j1}^t)} q(w | X_{tr,j1}^t, Z_{tr,j1}^t) p(b) db \\
&= \frac{1}{N_w} \sum_{k=1}^{N_w} \frac{l(Z_{tr,j1}^t | w_{j1,k}, b_k, X_{tr,j1}^t)}{p(Z_{tr,j1}^t | b_k, X_{tr,j1}^t)} \frac{p(w_{j1,k})}{q(w_{j1,k} | X_{tr,j1}^t, Z_{tr,j1}^t)} \delta(w - w_{j1,k}),
\end{aligned} \tag{22}$$

where the weight vectors $w_{j1,k}$ are now drawn from $q(w | X_{tr,j1}^t, Z_{tr,j1}^t)$, and the subscripts represent that each draw k depends on the $j1$ -th sample pair in the training dataset, $(X_{tr,j1}^t, Z_{tr,j1}^t)$, because the weight vectors have been trained.

From Eq. (22), we see that $p(w | X_{tr,j1}^t, Z_{tr,j1}^t)$ is represented by a set of weights $w_{j1,k}$, each with importance weight given as:

$$\beta_{j1,k} = \frac{1}{N_w} \frac{l(Z_{tr,j1}^t | w_{j1,k}, b_k, X_{tr,j1}^t)}{p(Z_{tr,j1}^t | b_k, X_{tr,j1}^t)} \frac{p(w_{j1,k})}{q(w_{j1,k} | X_{tr,j1}^t, Z_{tr,j1}^t)}. \tag{23}$$

Let us see if these importance weights $\beta_{j1,k}$ behave better than the $\alpha_{j1,k}$ in Eq. (21). The $\beta_{j1,k}$ consist of three factors that depend on the value of the weight vector. The prior $p(w)$ is typically a uniform distribution with an interval around zero, i.e., the probability $p(w_{j1,k})$ is the same for any drawn weight vector $w_{j1,k}$. The proposal density $q(w | X_{tr,j1}^t, Z_{tr,j1}^t)$ is the density of the trained weights. These trained weight vectors are obtained from samples of the prior density $p(w)$, and then transformed, via the minimization of a loss function, to the trained weights. Let us denote these prior weight vector samples as u_k and the trained weight vector samples as $w_{j1,k}$, to be able to clearly distinguish between them. We can write the transformation of the pdf of the prior weight vectors to that of the trained weight vectors using the standard transformation of variables formula from statistics, as:

$$q(w_{j1,k} | X_{tr,j1}^t, Z_{tr,j1}^t) = \left| \left(\frac{\partial w_{j1,k}}{\partial u_k} \right) \right|^{-1} p(u_k), \tag{24}$$

where $\left| \left(\frac{\partial w_{j1,k}}{\partial u_k} \right) \right|$ is the Jacobian of this transformation is a complicated function of u_k , and $w_{j1,k}$, and, specifically, will depend on k . This means that the proposal density values of the trained weights will not be equal to each other. This is also true for the likelihood values of the trained weights, meaning that the importance weights $\beta_{j1,k}$ will be different for each neural network defined by weight vector $w_{j1,k}$. Unfortunately, the differences in the $\beta_{j1,k}$ are huge, again leading to one importance weight having a value close to 1, while all others have values very close to zero. Since Bagging, Deep Ensembles and MC dropout use the trained weights in this way, they are of little value for providing information on $p(w | X_{tr,j1}^t, Z_{tr,j1}^t)$.

To avoid the issue mentioned above, we need to find a way to choose the proposal density $q(w | X_{tr,j1}^t, Z_{tr,j1}^t)$ such that all values of $\beta_{j,k}$ are the same. To achieve this goal, we first define a target likelihood value l_0 and find intermediate weight vectors $\tilde{w}_{j1,k}$, such that $l(Z_{tr,j1}^t | \tilde{w}_{j1,k}, b_k, X_{tr,j1}^t) = l_0$. Since all importance weight $\beta_{j1,k}$ are equal, it means that all the proposal density values $q(\tilde{w}_{j1,k} | X_{tr,j1}^t, Z_{tr,j1}^t)$ need to be equal as well. If we now look at the Jacobian of the transformation from the untrained to the trained weights, we need to calculate the variation of $\tilde{w}_{j1,k}$ by u_k . However, variations in $\tilde{w}_{j1,k}$ that reduce or increase $l(Z_{tr,j1}^t | \tilde{w}_{j1,k}, b_k, X_{tr,j1}^t)$ are not allowed, because the likelihood has to be fixed at $l(Z_{tr,j1}^t | \tilde{w}_{j1,k}, b_k, X_{tr,j1}^t) = l_0$. This means that the matrix $\left(\frac{\partial \tilde{w}_{j1,k}}{\partial u_k} \right)$ is not full rank, and hence its determinant $\left| \left(\frac{\partial \tilde{w}_{j1,k}}{\partial u_k} \right) \right| = 0$, such that the proposal density is not well defined. To avoid this issue, we define the final weight vectors in the proposal density by adding a small perturbation of size δ to each intermediate weight vector $\tilde{w}_{j1,k}$, as:

$$w_{j1,k} = \tilde{w}_{j1,k} + \delta B_{j1,k}(u_k), \quad (25)$$

where $B_{j1,k}(u_k)$ is a function of the untrained weight vector. The Jacobian can now be evaluated via a Taylor-series expansion around $\left| \left(\frac{\partial \tilde{w}_{j1,k}}{\partial u_k} \right) \right|$, and, since δ is small we only need to retain up to the first term in the expansion, leading to

$$\left| \left(\frac{\partial w_{j1,k}}{\partial u_k} \right) \right| = \left| \left(\frac{\partial \tilde{w}_{j1,k}}{\partial u_k} \right) + \delta \left(\frac{\partial B_{j1,k}}{\partial u_k} \right) \right| \approx \left| \left(\frac{\partial \tilde{w}_{j1,k}}{\partial u_k} \right) \right| + \delta \text{Tr} \left(\text{Adj} \left(\left(\frac{\partial \tilde{w}_{j1,k}}{\partial u_k} \right) \right) \left(\frac{\partial B_{j1,k}}{\partial u_k} \right) \right) + O(\delta^2), \quad (26)$$

where Tr denotes the trace, and Adj denotes the adjugate. If we now choose $\left(\frac{\partial B_{j1,k}}{\partial u_k} \right)$ as the pseudoinverse $\left(\frac{\partial B_{j1,k}}{\partial u_k} \right) = \left[\text{Adj} \left(\left(\frac{\partial \tilde{w}_{j1,k}}{\partial u_k} \right) \right) \right]^\dagger$ we find

$$\left| \left(\frac{\partial w_{j1,k}}{\partial u_k} \right) \right| \approx \left| \left(\frac{\partial \tilde{w}_{j1,k}}{\partial u_k} \right) \right| + \delta n + O(\delta^2) = \delta n + O(\delta^2), \quad (27)$$

where $n = \dim(w_{j1,k})$, and we used that $\left| \left(\frac{\partial \tilde{w}_{j1,k}}{\partial u_k} \right) \right| = 0$. This shows that, up to order δ , the Jacobian is a constant, independent of the weight vector $w_{j1,k}$. This, then, means that the proposal density $q(w_{j1,k} | X_{tr,j}^t, Z_{tr,j1}^t)$ has the same value for each weight vector $w_{j1,k}$.

However, by adding the small perturbation to the weight vectors, the likelihood is no longer equal to l_0 . We can perform a Taylor series expansion on the likelihood and find $l(Z_{tr,j1}^t | w_{j1,k}, b_k, X_{tr,j1}^t) = l_0 + \delta B_{j1,k} \nabla_{w_{j1,k}} l + O(\delta^2)$. The gradient of the likelihood is small, because the likelihood is close to its maximum due to the training. If a chosen δ is also small enough, we will have a very good approximation $l(Z_{tr,j1}^t | w_{j1,k}, b_k, X_{tr,j1}^t) = l_0$, such that we can ignore the change in the likelihood due to the perturbation, and that all weight vectors $w_{j1,k}$ will generate the same likelihood value.

The actual value for the likelihood l_0 is determined as follows. First, we train the NN with the unperturbed training data. This results in a weight vector, called w_0 . Then we use the N_{X1} perturbed training data and push each of them through the NN with weight vector w_0 . This will give rise to N_{X1} loss function values $J_{j1}(Z_{tr,j1}^t | X_{tr,j1}^t, w_0)$. We average these as $J_0 = \frac{1}{N_{X1}} \sum_{j1=1}^{N_{X1}} J_{j1}(Z_{tr,j1}^t | X_{tr,j1}^t, w_0)$ and take as target likelihood value $l_0 = \exp(-J_0)$. Since l_0 defined in this way is a representative likelihood value for trained weight vectors, the trained weight vectors based on the perturbed training data will form an unbiased sample from the posterior pdf of the weight vectors $p(w | X_{tr,j}^t, Z_{tr,j1}^t)$.

With the above choice of the weight vectors as $w_{j1,k} \approx \tilde{w}_{j1,k}$, we have ensured that the $q(w_{j1,k} | Z_{tr,j1}^t, X_{tr,j1}^t)$ are the same for each weight vector, and also that the $l(Z_{tr,j1}^t | w_{j1,k}, b_k, X_{tr,j1}^t)$ are the same for each weight vector. Hence, all importance weights $\beta_{j1,k}$ are the same. This means that the weight vectors are all equally probable in the posterior pdf of the weight vectors $p(w | X_{tr,j}^t, Z_{tr,j1}^t)$. With these equally probable samples from $p(w | X_{tr,j}^t, Z_{tr,j1}^t)$, Eq. (14) can be rewritten as:

$$p(z|x, \theta_{tr}, \theta_{te}) = \frac{1}{N_w} \sum_{k=1}^{N_w} \frac{1}{N_x} \sum_{i=1}^{N_x} \frac{1}{N_{X1}} \sum_{j1=1}^{N_{X1}} \frac{1}{N_{X2}} \sum_{j2=1}^{N_{X2}} p(z|w_{j1,k}, x_i^t, X_{te,j2}^t, Z_{te,j2}^t). \quad (28)$$

3.4 Source 4: Uncertainty in the trained NN

As shown in Eq. (28), the final step is to estimate $p(z|w_{j1,k}, x_i^t, X_{te,j2}^t, Z_{te,j2}^t)$, the uncertainty due to an imperfect NN. The imperfectness is evaluated using the testing data $(X_{te,j2}^t, Z_{te,j2}^t)$ for each $j2$. Since the evaluation is based on the statistical relation described by the input-output pairs of testing data, we rewrite $p(z|w_{j1,k}, x_i^t, X_{te,j2}^t, Z_{te,j2}^t) = p_{\theta_{te,j2}}(z|w_{j1,k}, x_i^t)$, i.e. the pdf of z given the input x_i^t and weight vector $w_{j1,k}$, determined using the input-output pairs in the testing data $j2$ for which the input testing data is close to x_i^t . If we denote the area around x_i^t in the testing data as $D_{x_i^t}$, we find:

$$p_{\theta_{te,j2}}(z|x_i^t, w_{j1,k}) = \pi(Z_{te,j2,m}|w_{j1,k}, X_{te,j2,m}, m \text{ such that } X_{te,j2,m} \in D_{x_i^t}) \quad (29)$$

in which π means a representation of the pdf, based on elements m of the output testing data vector $Z_{te,j2}$ in which m is such that $(X_{te,j2,m} \in D_{x_i^t})$. This representation can be a pdf approximated by known functions (e.g., a Gaussian or a Gaussian mixture), a histogram, the set of samples $Z_{te,j2,m}$, or by new samples generated from $Z_{te,j2,m}$ (e.g., via a so-called diffusion process; see Sohl-Dickstein et al., 2015). The size of $D_{x_i^t}$, the area in which input testing data are considered close to x_i^t , is related to the uncertainty in the input testing data. In our experience, values chosen between 0.5 and 2 times the uncertainty standard deviation in the input testing data lead to very similar output pdfs.

3.5 The resulting algorithm and practical considerations

Using Eq. (29) into Eq. (28), we have a complete uncertainty quantification methodology, that can be written as:

$$p(z|x, \theta_{tr}, \theta_{te}) = \frac{1}{N_w} \sum_{k=1}^{N_w} \frac{1}{N_x} \sum_{i=1}^{N_x} \frac{1}{N_{X1}} \sum_{j1=1}^{N_{X1}} \frac{1}{N_{X2}} \sum_{j2=1}^{N_{X2}} p_{\theta_{te,j2}}(z|x_i^t, w_{j1,k}). \quad (30)$$

This equation shows that we average the pdfs $p_{\theta_{te,j2}}(z|x_i^t, w_{j1,k})$, determined by each testing data set $j2$, over the input samples i , the trained weight vector samples k , the training data samples $j1$, and the testing data samples $j2$ to find the full uncertainty pdf of the output of the deep learning procedure. A practical algorithm is as follows:

1. Train an NN in the standard way not perturbing any input training data, using a method to avoid overfitting, but not dropout, and store the resulting weight vector w_0 .
2. Generate an ensemble of size N_{X1} of **training** data vectors $Z_{tr,j1}^t X_{tr,j1}^t$ $j1 = 1, 2, \dots, N_{X1}$, drawn from the uncertainty distributions of the input and output training vectors. This results in a very large data set as this generates N_x perturbed copies of the full training data vector. We have used $N_x = 20$ which gives nearly identical results to $N_x = 10$ in our example below, but this should be tested in other applications. As mentioned at the end of section 3.3, if the likelihood is Gaussian and the output training data are also Gaussian distributed, we do not have to perturb the output training data.
3. Determine the target likelihood value l_0 . Use the perturbed input training data $X_{tr,j1}^t$, with $j1 = 1, 2, \dots, N_{X1}$ to evaluate the loss function value using the weight vector w_0 **that we already calculated in step 1**:

$$J_{j1}(Z_{tr,j1}^t | X_{tr,j1}^t, w_0) = \frac{1}{2} \sum_{m=1}^{N_{X1}} \left(Z_{tr,j1,m}^t - f(X_{tr,j1,m}^t, w_0) \right)^2 \quad (31)$$

for each $j = 1, 2, \dots, N_{X1}$, where we used that the training and testing data have been normalized, so all have standard deviations are equal to 1. Set the target loss function value to $J_0 = \frac{1}{N_{X1}} \sum_{j1=1}^{N_{X1}} J_{j1}(Z_{tr,j1}^t | X_{tr,j1}^t, w_0)$, so J_0 is the mean value of evaluating the loss function for each of the perturbed training sets from step 2). To this target loss function value corresponds the target likelihood value $l_0 = \exp(-J_0)$. (If the likelihood is Gaussian and the output training data are also Gaussian distributed, we do not have to perturb the output training data.)

4. Determine an ensemble of weight vectors. Train $N_{X1} \times N_w$ neural networks, that differ in training data (step 2), and in initial untrained weight vectors and batch orders (N_w). We took $N_w = 20$ in our example below, but sensitivity should be tested for other applications. These networks should all be trained such that their loss function value is close to the target loss function value, i.e.

$$J_{j1}(Z_{tr,j1}^t | X_{tr,j1}^t, w_{j1,k}, b_k) = J_0 \quad (32)$$

This doesn't have to be exact, but it must be quite close. As a rule of thumb, the difference from J_0 should be smaller than 0.01. Then calculate the likelihood value for each of them as

$$l_{j1}(Z_{tr,j1}^t | X_{tr,j1}^t, w_{j1,k}, b_k) = \exp[-J_{j1}(Z_{tr,j1}^t | X_{tr,j1}^t, w_{j1,k}, b_k)] \quad (33)$$

Since the loss function values are so large due to the large number of training and testing pairs, all likelihood values will be zero in the computer because of round-off errors. However, we only need to know the likelihood value relative to the other likelihood values. Hence, we can subtract J_0 from each J_j value before the exponent is calculated, avoiding the round-off errors.

5. Generate N_x perturbed values for the new input vector, and push each of them through the $N_{X1} \times N_w$ neural networks from step 5. This will give rise to $N_x \times N_{X1} \times N_w$ outputs of neural networks.
6. Generate an ensemble of size N_{X2} of input **testing** data vectors $Z_{te,j2}^t X_{te,j2}^t$ $j = 1, 2, \dots, N_{X2}$, drawn from the uncertainty distribution of the testing data. This results in N_{X2} perturbed copies of the testing data. We took $N_{X2} = 20$ in our example below, but sensitivity should be tested for other applications.
7. Take into account the uncertainty in the neural networks. Use the ensemble of testing data $Z_{te,j2}^t X_{te,j2}^t$ to determine $p_{\theta_{te,j2}}(z | x_i^t, w_{j1,k}, b_k)$ for each $i, k, j1$, and $j2$, using only the output testing data $Z_{te,j2}^t$ that correspond to those input testing data in $X_{te,j2}^t$ that are close to x_i^t . Average these $N_x \times N_w \times N_{X1} \times N_{X2}$ pdfs to find the final uncertainty pdf for output z .

Note that the above algorithm can be simplified if $l(Z_{tr,j1}^t | w_{j1,k}, b_k, X_{tr,j1}^t)$ is assumed to be Gaussian as in Eq. (19), and the uncertainty in the output training data Z_{tr} is also Gaussian distributed. In that case, we do not need to introduce Z_{tr}^t and draw samples from $p(Z_{tr}^t | Z_{tr})$ in Step 2. Instead, we can work directly with $p(w | X_{tr,j1}^t, Z_{tr})$. Then the likelihood of the weight vectors becomes:

$$l(Z_{tr}|w, b, X_{tr,j1}^t) = A \cdot \exp \left[-\frac{1}{2} \sum_{m=1}^{N_{tr}} \frac{(Z_{tr,m} - f(X_{tr,j1,m}^t, w, b))^2}{\sigma_f^2 + \sigma_{z,m}^2} \right],$$

in which $\sigma_{z,m}^2$ is the uncertainty variance in the output training data $Z_{tr,m}$. Everything from Eq (19) to Eq. (28) remains the same, with that difference that $Z_{tr,j1}^t$ is replaced everywhere with Z_{tr} . This is a situation often encountered in the geosciences, we will use this formalism in our example in Section 4.

4. Application to predictions of cloud process rate

In this section, we apply our methodology to quantify uncertainty in rates of autoconversion, a critical process that describes the formation of rain droplets through cloud droplet collision-coalescence. The importance and the stochastic nature of the autoconversion process make it a perfect machine learning application (Chiu et al., 2021; Gettelman et al., 2021).

4.1 Description of the training and testing datasets

In this example, we capitalize on the training and testing datasets and the machine learning model built in Chiu et al. (2021). The datasets were derived based on aircraft cloud probe measurements in the Aerosol and Cloud Experiments in the Eastern North Atlantic (ACE-ENA) field campaign, and the stochastic collection equation formulated as a two-moment bin model. The Artificial Neural Network comprises six hidden, fully connected layers with 16 nodes in each layer. The input vector has four elements, namely cloud water content (q_c), cloud droplet number concentration (N_c), drizzle water content (q_r), and drizzle drop number concentration (N_r) with uncertainty of 30%, 50%, 30%, and 20%, respectively (Glienke & Mei, 2019, 2020; Mei et al., 2020). The output autoconversion rate varies from 7.7×10^{-24} to $2.8 \times 10^{-6} \text{ kg m}^{-3} \text{ s}^{-1}$, providing a large range of experimental conditions for this study. The data obtained were divided in training, validation, and testing data with sample sizes of 6,325,526, 2,140,727, and 2,145,571, respectively. We took the \log_{10} of all training and testing data to reduce the spread and to obtain additive Gaussian uncertainties.

4.2 Training procedure

Following the procedure summarized in Section 3.5, we trained the first NN using the unperturbed training data with randomly chosen initial weight vector and batch order, and followed the early stopping approach (Prechelt, 1998) to avoid overfitting. The training is stopped when the loss function from the validation dataset no longer decreases when an additional epoch of the training dataset is supplied to the NN. Because the loss function values of the validation dataset vary significantly with epoch, we smoothed the lost function values for the validation data by a moving average over 50 epochs. For convenience, we denote the trained weight vector resulted from the first NN as w_0 .

We assumed Gaussian uncertainties on the output training data, such that we do not have to sample from $p(Z_{tr}^t|Z_{tr})$, see the description at the end of Section 3.5. Next, we draw 20 input training data sets from $p(X_{tr}^t|X_{tr})$, using the uncertainty characteristics from Section 4.1. Hence, $N_{X1} = 20$. For each of those datasets, we made predictions using w_0 and computed the corresponding loss function values from Eq. (31), and set the mean of these lost function values as the target loss function value J_0 (see Eq. (32)). Then, we trained the weight vectors for each of these 20 perturbed input training datasets $X_{tr,j1}^t$, and with 20 sets of perturbed initial weights and batch orders ($N_w = 20$). We stopped the training for each of them when the lost function values from the training data reached J_0 . As a result, we obtained $20 \times 20 = 400$ NN for quantifying the uncertainty in the weights and in the training data.

Using J_0 poses a practical issue. Many machine learning codes report loss function values only at the end of a full epoch. Hence, stopping the training when the exact value for J_0 is reached is not trivial. We handled this by first finding the two

epochs that comprise a range of loss function values where J_0 falls between. Then we used simple bisection to find a full loss function value that agrees to J_0 within 0.01. This threshold leads to likelihood values that are sufficiently close to $l_0 = \exp(-J_0)$, such that the importance weights are similar in all 400 NNs. As shown in Fig. 1, most importance weights are close to the expected value of $1/400=0.0025$ for a perfect equal-weight ensemble. However, while this procedure worked well for most of the 400 NNs, a few did not converge. This is not surprising since we are performing bisection in a very high-dimensional space. For those NNs, we stopped at lost function values that have larger differences from J_0 . The resulting importance weights for those NNs do not deviate too much from 0.0025 (only by 6% as shown in Fig.1), which still fulfills the need of almost equal importance weights for our methodology.

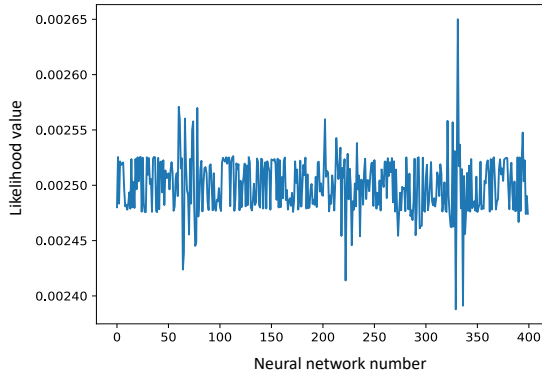


Figure 1. The normalized likelihoods (i.e., the importance weights) for the 400 NN's.

4.3 Results

To test our methodology with new input data, we used 50 different input vectors to cover a large range of input values. Each was perturbed 100 times by a random vector drawn from the uncertainty pdf of input variables described in Section 4.1. For each input x , this procedure results in 40,000 samples ($N_x = 100$, $N_w = 20$, $N_{x1} = 20$). Using the testing data, we calculated the uncertainty pdf for each of those, as in Eq. (29), and averaged the resulting histograms. As mentioned in Section 3.4, we need to determine the area ($D_{x_i^t}$) in the training data around the sample x_i^t , which depends on how we define the closeness of the input testing data to x_i^t . We used all output testing data that had corresponding input testing data close to x_i^t within 0.2 (in \log_{10} space), for each of the four elements of the input vector. Experimentation with larger values up to 0.5, or smaller values down to 0.1 did not lead to visual differences in the pdfs.

The results for all 50 input vectors are displayed in Appendix B. To highlight the key findings, Fig. 2 shows the total uncertainty pdfs as a function of the \log_{10} of the autoconversion rate for four different input vectors x . In each plot, the blue curve is the total uncertainty pdf from Eq. (30), and the red bar is the autoconversion rate predicted by the traditional neural network (i.e., w_0) without uncertainty quantification. The black bars are the output samples generated using Bagging, defined here as generating an ensemble of neural networks, of size 20 in this case, by perturbing the initial weight vectors and batch order. This results in 20 samples to describe the uncertainty according to Bagging.

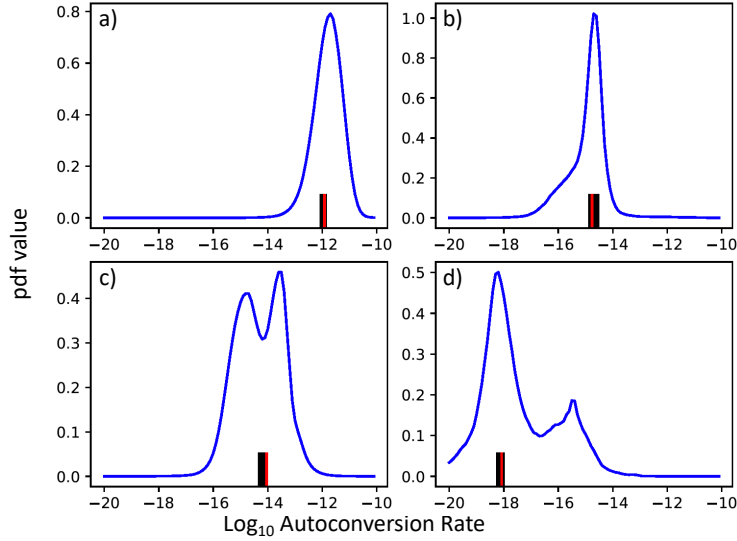


Figure 2. Examples of total uncertainty pdf in the output autoconversion rate for four input vectors. The blue curves are the total uncertainty pdfs, the red bar is the autoconversion rate calculated by traditional deep learning without uncertainty quantification. The black bars are the output samples generated using Bagging and used as a measure of uncertainty for the Bagging approach. Note the wide variety of shapes of the blue uncertainty pdfs and the small spread in the black bars, demonstrating the inadequacy of the Bagging approach to represent uncertainty (see discussion in text).

Figures 2(a) and (b) show that the width of the pdfs is about a factor of 10 in autoconversion rate, and sometimes more, which is not surprising given the relatively large measurement uncertainty in the input variables (ranging between 20% and 50%). Although the pdf in Fig. 2(a) can be approximated by a Gaussian distribution, a non-negligible skewness is observed in Fig. 2(b). The pdfs in Fig. 2(c) and (d) are wider, showing large uncertainty and bimodality in the pdfs.

To understand the relative contribution of the different uncertainty sources to the final uncertainty estimate, and the origin of the bimodality in Fig. 2(c) and (d), we first calculated the uncertainty only due to the weights. This is done by removing the uncertainty in the new input vector, the training and the testing data, and the NN from Eq. (30) and by removing the summations over i , $j1$, and $j2$, and replacing the pdfs $p_{\theta_{te,j2}}(z|x_i^t, w_{j1,k})$ with the samples generated from using the ensemble of weight vectors. The resulting uncertainty ensemble is very narrow, similar to the black bars in Fig. 2, indicating that the uncertainty in the weights is not a dominant source in this data set. Second, we isolated the output uncertainty due to the uncertainty in the input vector x , and due to the NN as determined via the testing data (the pdfs $p_{\theta_{te,j2}}(z|x_i^t, w_{j1,k})$) by removing the summations over those uncertainty sources that are now kept fixed in Eq. (30). We found that the contributions from these two sources have similar magnitudes. As shown in Fig. 3, the combined influence from these two sources (i.e., the black lines) typically peaks at the same location as the full uncertainty pdf (i.e., the blue lines), highlighting their significant contributions to the total output uncertainty. However, interestingly, the combined uncertainty from these two sources is typically unimodal and symmetric (in the \log_{10} space), and cannot represent the second mode and skewness seen in the total uncertainty pdf. This suggests that the strong skewness and bimodal feature in the total uncertainty pdf is related to the uncertainty in training and testing data.

To understand the reason for skewness and bimodal features in some final uncertainty pdfs, we analyzed all cases (see Appendix B) and found that positive skewness is only observed for high autoconversion values of larger than about 10^{-12} , while high negative skewness values are found for intermediate autoconversion values (10^{-17} to 10^{-14}). Low autoconversion values (around 10^{-18}) tend to show bimodal behavior. We looked into the testing data in detail, with an attempt to connect input values with output skewness and bimodality, but were unsuccessful due to the difficulty in visualizing the 4-dimensional

input space. Unfortunately, any 3-dimensional plot of three of the four input variables also did not reveal any particular structure to allow us to provide further insights.

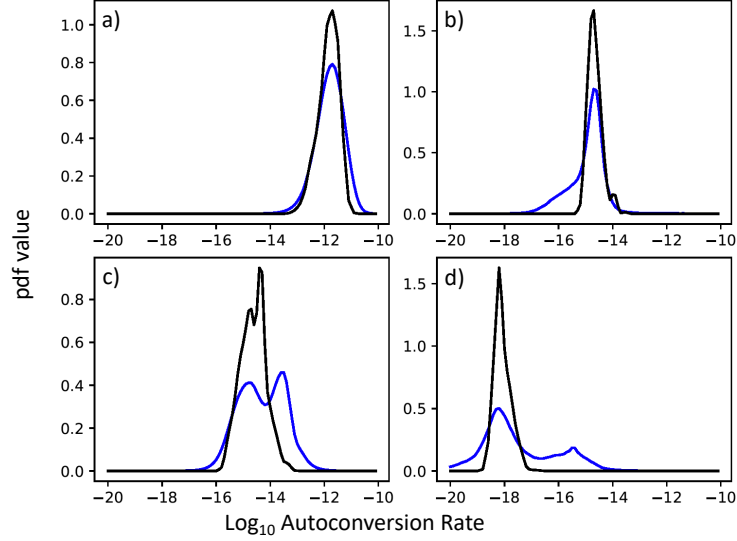


Figure 3. Same as Fig. 2, but shows the blue curves that represent the uncertainty pdfs considering all uncertainty sources, and adds the black curves that are derived considering the uncertainty in the new input vector and the uncertainty in the neural network only.

Back to Fig. 2, we see the inadequacy of the Bagging approach for this example. The black bars cover a very small interval, leading to a substantial underestimation of the uncertainty. Additionally, bimodality is not observed for Bagging in this example. In fact, Bagging performs even worse than displayed here. As explained in Section 3.3, the discussion directly below Eq. (21), one cannot just take an ensemble of fully trained neural networks and use each of them as being equally likely. Their relative weight, or importance weight, is determined by their likelihood values, hence by the exponent of the loss function values. Since the importance weights sum to one, it is only the ratio of the likelihoods that plays a role in the importance weights. To illustrate the point, we divided each likelihood value by the largest likelihood value. The result is that one neural network gets an importance weight of 1, and all other importance weights will be smaller. In our example, the next highest importance weight is $\exp(-824)$, which is an extremely small number compared to one. The other importance weights are even smaller. These are the importance weights that should be used by methods such as Bagging, Deep Ensembles, and MC Dropout. We see that only the weight vector with the highest importance weight remains, and all other weight vectors have a negligible contribution to the uncertainty pdf and should be discarded. These numbers should be compared with our nearly equal importance weights in Fig 1. We can thus conclude that if methods like Bagging, Deep Ensembles, and MC Dropout were used in a statistically consistent way, they would be just a waste of time, because only one ensemble member remains, and, because of this, the uncertainty in the output of that neural network cannot be determined.

5. Conclusions and discussion

Uncertainty quantification of deep learning results in the geosciences is crucial for their scientific use, and for full acceptance of the machine learning methodology. We summarized the literature and demonstrated where shortcuts and approximations are typically made in existing methods for uncertainty quantification, and which uncertainty sources are ignored. Since the existing methods are either incomplete or inaccurate, we developed a systematic way to calculate output uncertainty, taking all possible sources of uncertainty into account. These sources are uncertainty in 1) the input values, 2) the training and testing

data, 3) the weight vectors related to uncertainty in initial weight vectors and the batch order, and 4) the resulting neural network, as established via the testing dataset. Our methodology is general since it makes no assumptions on the relative importance of the four uncertainty sources. It is expected that this methodology will bring machine learning on a proper scientific footing, and help acceptance of machine learning techniques in the geosciences.

Additionally, we provided a practical way to implement the methodology and analyzed the contribution of each uncertainty source for a real-world example. In this example, cloud autoconversion rates were predicted using deep learning trained by the stochastic collection equation formulated as a two-moment bin model and aircraft cloud probe measurements from the Aerosol and Cloud Experiments in the Eastern North Atlantic (ACE-ENA) field campaign, deployed by the Atmospheric Radiation Measurement (ARM) user facility. We showed that the dominant source of output uncertainty in this example comes from uncertainty in the training and testing data sets, resulting in about a factor of 10 or more in output uncertainty, but uncertainty in the new input vector and uncertainty from each neural network as determined from testing data cannot be ignored at about half that value. The uncertainty from the initial weight vector values and the batch order during training typically contributes the least to the final uncertainty pdf in our example.

We compared our results with methods that generate an output ensemble via a weight vector ensemble, such as Bagging, Deep Ensembles and MC dropout. However, the ensemble members generated via those methods are not properly weighted by their likelihood values, as a consistent application of statistics dictates. When this so-called importance weighting is applied, one ensemble member will have a much larger importance weight than all the others, effectively reducing the ensemble to just one member. Based on this, such methods in their basic implementation cannot be used for uncertainty quantification.

When the new input data falls outside the training and testing data set, deep learning can provide unexpected or even completely wrong output for such input data. This introduces an extra source of uncertainty, which is not included in our methodology because it cannot be quantified in a principled way. Two methodologies can be used to reduce the sensitivity of the NN to these outliers and alleviate this issue. The first is to make the trained machine more robust by generating extra training data that cover a larger part of state space. Some methods have been proposed, e.g., using symmetries in training data (e.g., Yu and Ma, 2021). Our methodology automatically generates extra training and testing data, but does this in a principled way by perturbing these datasets within their uncertainty as part of the uncertainty quantification. The second methodology is to include extra prior knowledge in the optimization, for instance, extra constraints that enforce physical consistency. Bayes Theorem provides a systematic way to add such extra prior information. Since our methodology is based on Bayes Theorem, including such extra constraints fit perfectly into our uncertainty framework and it would be straightforward in practical implementation.

Appendix A: The uncertainty in the input training data

In this appendix we provide an extended discussion of how one can treat uncertainty in input training data in the machine-learning likelihood. We denote the input training data as X , and the output training data as Z for ease of notation. Also, we suppress the batch order in the NN function. Following the main text, we introduce the possible true input data as a random variable X^t , and write:

$$\begin{aligned} p(Z|X, w) &= \int p(Z, X^t|X, w) dX^t = \\ &= \int p(Z|X^t, w) p(X^t|X) dX^t = \int p(Z|X^t, w) p(X^t|X) dX^t \end{aligned} \quad (\text{A.1})$$

where we used that the input data depends not on the weight vector, and that, with X^t given, X does not provide extra information on Z . The pdf $p(X^t|X)$ is the pdf that describes the uncertainty in the input training data. For the other pdf, $p(Z|X^t, w)$, we use the fact that the weight vector w is given, which means that the output training data Z are assumed to be generated via a neural network with that weight vector, applied to the input training data X^t . In general, there will be uncertainty in the output training data and the NN will not be perfect, so that we can write for each training pair m :

$$Z_m = f(X_m^t, w) + \varepsilon_m(X_m^t) \quad (\text{A.2})$$

in which $\varepsilon_m(X_m^t)$ denotes the uncertainty in the output training data Z_m and in the NN, which can depend on the input data value X_m^t . This equation shows that the uncertainty pdf of output training data given X^t and w , so the pdf $p(Z|X^t, w)$, is the same as the pdf of $\varepsilon(X^t)$ but shifted by the value $f(X^t, w)$. We used the same argument in Section 3.3, but note that we are now discussing uncertainty in training data, not the result of a new input value.

As an example, if we assume that the uncertainties in the output data and the NN are *independent* Gaussian distributed, with variances $\sigma_{z,m}^2$ and σ_f^2 , respectively, we can write:

$$p(Z_m|X_m^t, w) = p_\varepsilon(\varepsilon_m(X_m^t)) = A \exp \left[-\frac{1}{2} \frac{\varepsilon_m^2(X_m^t)}{\sigma_f^2 + \sigma_{z,m}^2} \right] = A \exp \left[-\frac{1}{2} \frac{(Z_m - f(X_m^t, w))^2}{\sigma_f^2 + \sigma_{z,m}^2} \right] \quad (\text{A.3})$$

in which A is a normalization factor and $\sigma_f^2 + \sigma_{z,m}^2$ is the variance of the uncertainty variable $\varepsilon_m(X_m^t)$. The independence assumption is not essential, and we refer to e.g. the data assimilation literature, such as Evensen et al. (2022), on how to include dependencies in the uncertainties, but that is not the main point here. If we now also assume that the uncertainty in the input training data $p(X^t|X)$ is independent Gaussian, we find for the pdf for each training pair m , using Eq. (B.1):

$$p(Z_m|X_m, w) = A \int \exp \left[-\frac{1}{2} \frac{(Z_m - f(X_m^t, w))^2}{\sigma_f^2 + \sigma_{z,m}^2} - \frac{1}{2} (X_m^t - X_m)^T C_m^{-1} (X_m^t - X_m) \right] dX_m^t \quad (\text{A.4})$$

in which A is another normalization factor and the input X_m is allowed to be a vector with uncertainty covariance C_m . (The independency is between input-output samples, not necessarily between the elements of an input sample.) Evaluating this integral is cumbersome because $f(X_m^t, w)$ is a highly nonlinear function. However, when the uncertainty in the input data is small, such that we can approximate:

$$f(X_m^t, w) \approx f(X_m, w) + F_m(X_m^t - X_m) \quad (\text{A.5})$$

in which F_m is the local derivative of the nonlinear function f at input vector value X_m , we can evaluate the integral because its argument is now the product of two Gaussians in the integration variable X_m^t . We then find:

$$p(Z_m|X_m, w) = A_m \exp \left[-\frac{1}{2} \frac{(Z_m - f(X_m, w))^2}{\sigma_f^2 + \sigma_{z,m}^2 + F_m C_m F_m^T} \right] \quad (\text{A.6})$$

leading to, for all N_x input data:

$$p(Z|X, w) = \prod_{m=1}^{N_x} p(Z_m|X_m, w) = A \exp \left[-\frac{1}{2} \sum_{m=1}^{N_x} \frac{(Z_m - f(X_m, w))^2}{\sigma_f^2 + \sigma_{z,m}^2 + F_m C_m F_m^T} \right] \quad (\text{A.7})$$

in which A is yet another normalization constant. We conclude that, if the uncertainty in the input data is small, such that a linearization of the network around this input value makes sense, then we recover the standard deep learning likelihood, but now the uncertainty in that likelihood contains the sum of the output uncertainty, NN uncertainty, and the input uncertainty transformed to output space via the linearized NN (the $F_m C_m F_m^T$ term).

When the uncertainties are not Gaussian, or when the linearization of the NN is not accurate, analytical solutions quickly become impossible. In that case we can use Monte-Carlo methods to evaluate the integral (B.1). The idea is to draw N_x samples from $p(X_m^t|X_m)$. This means that we represent $p(X_m^t|X_m)$ by a set of delta functions, each centered on a sample $X_{m,j}^t$, as:

$$p(X_m^t|X_m) = \frac{1}{N_x} \sum_{j=1}^{N_x} \delta(X_m^t - X_{m,j}^t) \quad (\text{A.8})$$

If we use this in Eq. (B.1), together with Eq. (B.3), we find for each training pair m :

$$p(Z_m|X_m, w) = A \frac{1}{N_x} \sum_{j=1}^{N_x} \exp \left[-\frac{1}{2} \frac{(Z_m - f(X_{m,j}^t, w))^2}{\sigma_f^2 + \sigma_{z,m}^2} \right] \quad (\text{A.9})$$

such that

$$p(Z|X, w) = A \frac{1}{N_x} \sum_{j=1}^{N_x} \exp \left[-\frac{1}{2} \sum_{m=1}^N \frac{(Z_m - f(X_{m,j}^t, w))^2}{\sigma_f^2 + \sigma_{z,m}^2} \right] \quad (\text{A.10})$$

which is what we used in the main text.

Appendix B: Full results

The following figures show the full uncertainty pdfs for all 50 new input values (blue curves), the uncertainty due to input uncertainty and the uncertainty of the network as determined from the testing data (black curves), the unperturbed autoconversion estimate (red bar) and the uncertainty estimate from the weight uncertainty only (black bars), but omitting the importance weights, see main text.

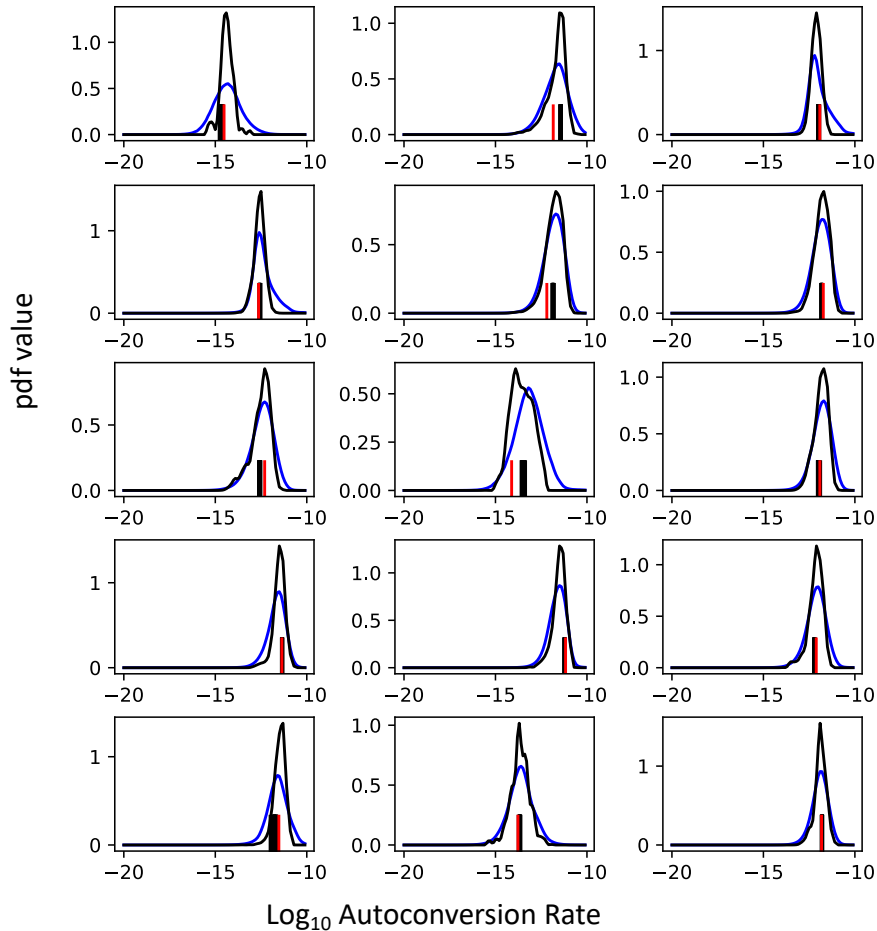


Figure B1. Examples of total uncertainty pdf in the output autoconversion rate for 50 input vectors. The blue curves are the total uncertainty pdfs, black curves that are derived considering the uncertainty in the new input vector and the uncertainty in the neural network only. the red bar is the autoconversion rate calculated by traditional deep learning without uncertainty quantification. The black bars are the output samples generated using Bagging and used as a measure of uncertainty for the Bagging approach.

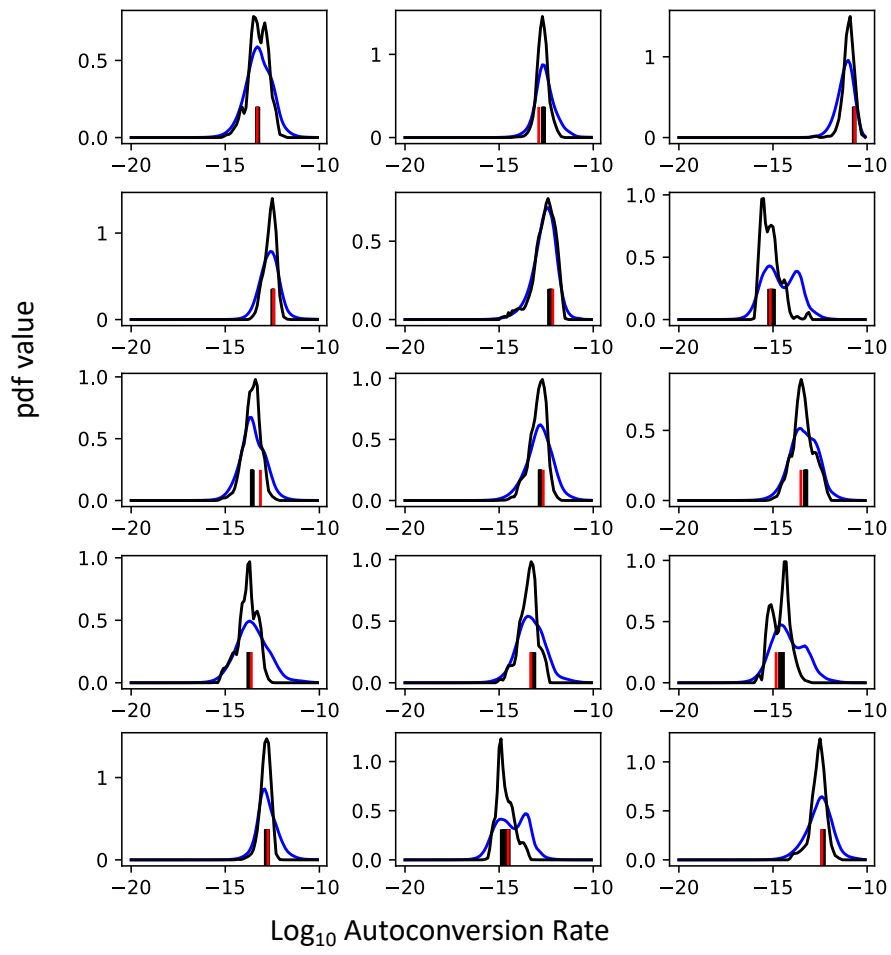


Figure B1 (continued)

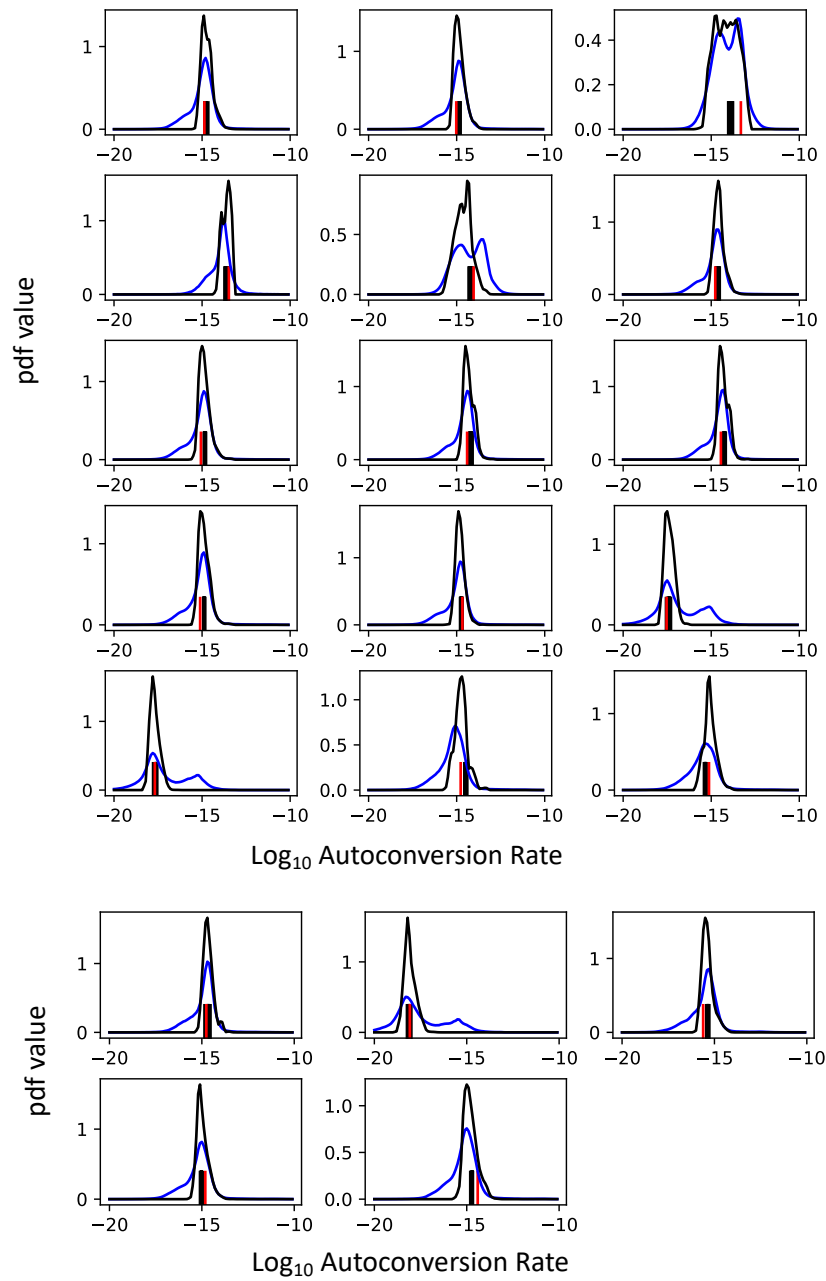


Figure B1 (continued)

Author contribution: PJvL and JCC developed the idea, prepared the manuscript, and acquired the funding. PJvL developed the methodology, performed the formal analysis, and developed the figures. CKY performed the numerical experiments.

Competing interests: The authors declare that they have no conflict of interest.

Acknowledgements: Van Leeuwen was supported by the National Science Foundation under Grant 2220201. Chiu and Yang were supported by Department of Energy under Grant DE-SC0021167, and National Aeronautics and Space Administration Projects 80NSSC22K1546 and 80NSSC23K1017.

References

- Abdar, M., F. Pourpanah, S. Hussain, D. Rezazadegan, L. Liu, M. Ghavamzadeh, P. Fieguth, X. Cao, A. Khosravi, U. R. Acharya et al., (2021) A review of uncertainty quantification in deep learning: Techniques, applications and challenges, *Information Fusion*, vol. 76, pp. 243–297, doi:10.1016/j.inffus.2021.05.008.
- Ades, M., and P.J. Van Leeuwen (2012), An exploration of the Equivalent-Weights Particle Filter, *Q. J. Royal Meteorol. Soc.*, doi:10.1002/qj.1995.
- Andrieu, C., N. de Freitas, A. Doucet, M. Jordan (2003) An Introduction to MCMC for Machine Learning. *Machine Learning*, 50, 5–43, doi:10.1023/A:1020281327116
- Beheng, K. D. (1994). A parameterization of warm cloud microphysical conversion processes. *Atmospheric Research*, 33, 193–206.
- Blundell, C., Cornebise, J., Kavukcuoglu, K., and Wierstra, D. Weight Uncertainty in Neural Network. In *International Conference on Machine Learning*, pp. 1613–1622, June 2015.
- Breiman, L. (1996) Bagging Predictors, *Machine Learning*, 24, doi:10.1007/BF00058655.
- Cheng, S.B., C. Quilodrán-Casas, S. Ouala, A. Farchi, C. Liu, P. Tandeo, R. Fablet, D. Lucor, B. Iooss, J. Brajard, D. H. Xiao, T. Janjic, W. P. Ding, Y. K. Guo, A. Carrassi, M. Bocquet, and R. Arcucci, Machine learning with data assimilation and uncertainty quantification for dynamical systems: A review, *IEEE/CAA J. Autom. Sinica*, vol. 10, no. 6, pp. 1361–1387, Jun. 2023. doi: 10.1109/JAS.2023.123537.
- Chiu, C., C. K. Yang, P. J. van Leeuwen, G. Feingold, Robert Wood, Yann Blanchard, Fan Mei, Jian Wang (2020) Observational Constraints on warm cloud microphysical processes using machine learning and optimization techniques, *Geophys. Res. Lett.*, doi: 10.1029/2020GL091236
- Evensen, G., F.M. Vossepoel, and P.J. van Leeuwen (2022) *Data Assimilation Fundamentals*, Springer, **open access**, doi: 10.1007/978-3-030-96709-3
- Gal, Y. and Ghahramani, Z. Dropout As a Bayesian Approximation: Representing Model Uncertainty in Deep Learning. In *Proceedings of the 33rd International Conference on International Conference on Machine Learning*, volume 48 of *ICML’16*, pp. 1050–1059, New York, NY, USA, 2016.
- Glienke, S., & Mei, F. (2019). Two-dimensional stereo (2D-S) probe instrument handbook. Retrieved from https://www.arm.gov/publications/tech_reports/handbooks/doe-sc-arm-tr-233.pdf
- Glienke, S., & Mei, F. (2020). Fast cloud droplet probe (FCDP) instrument handbook. Retrieved from https://www.arm.gov/publications/tech_reports/handbooks/doe-sc-arm-tr-238.pdf
- Golaz, J.-C., Horowitz, L. W., & Levy, H. II (2013). Cloud tuning in a coupled climate model: Impact on 20th century warming. *Geophysical Research Letters*, 40, 2246–2251. <https://doi.org/10.1002/grl.5023>.
- Goodfellow, I, Y. Bengio, and A. Courville (2016) *Deep Learning*, MIT Press, ISBN 9780262035613.

- Lakshminarayanan, B., A. Pritzel, and C. Blundell, (2017) Simple and scalable predictive uncertainty estimation using deep ensembles, *Advances in neural information processing systems*, 30.
- MacKay, D. J. C. (1992) A Practical Bayesian Framework for Backpropagation Networks. *Neural Computation*, 4, 448–472, doi: 10.1162/ neco.1992.4.3.448.
- Mei, F., Wang, J., Comstock, J. M., Weigel, R., Kr. mer, M., Mahnke, C., et al. (2020). Comparison of aircraft measurements during GoAmazon2014/5 and ACRIDICON-CHUVA. *Atmospheric Measurement Techniques*, 13, 661–684. doi:10.5194/amt-13-661-2020
- Miller, B. B. and Carter, C. (2015) The test article, *J. Sci. Res.*, 12, 135–147, doi:10.1234/56789.
- Nix, D. A., and A. S. Weigend, (1994) Estimating the mean and variance of the target probability distribution, *Proceedings of 1994 IEEE International Conference on Neural Networks (ICNN'94)*, Orlando, doi: 10.1109/ICNN.1994.374138.
- Osband, I. Risk versus Uncertainty in Deep Learning: Bayes, Bootstrap and the Dangers of Dropout. In *NIPS 2016 Workshop on Bayesian Deep Learning*, Barcelona, Spain, October 2016.
- Neal, R. M. (1996) *Bayesian Learning for Neural Networks*, *Lecture Notes in Statistics* 118, Springer, doi:10.1007/978-1-4612-0745-0
- Pfreundschuh, S., Eriksson, P., Duncan, D., Rydberg, B., Håkansson, N., and Thoss, A.: A neural network approach to estimating a posteriori distributions of Bayesian retrieval problems, *Atmos. Meas. Tech.*, 11, 4627–4643, doi:10.5194/amt-11-4627-2018, 2018
- Prechelt, L. (1998) Automatic Early Stopping Using Cross Validation: Quantifying the Criteria. *Neural Networks*, 11, 761–767, doi:10.1016/S0893-6080(98)00010-0
- Smith, A. A., C. Carter, and B. B. Miller (2014) More test articles, *J. Adv. Res.*, 35, 13–28, doi:10.2345/67890.
- Sønderby, C. K., L. Espeholt, J. Heek, M. Dehghani, A. Oliver, T. Salimans, S. Agrawal, J. Hickey, N. Kalchbrenner (2020) *MetNet: A Neural Weather Model for Precipitation Forecasting*, Google research, arXiv:2003.12140v2 (not reviewed).
- Sohl-Dickstein, J., E. Weiss, N. Maheswaranathan, and S. Ganguli (2015) Deep unsupervised learning using nonequilibrium thermodynamics. In: *Proceedings of Machine Learning Research* 37, pp 2256–2265, Available from <https://proceedings.mlr.press/v37/sohl-dickstein15.html>
- Stephens, G. L., L'Ecuyer, T., Forbes, R., Gettleman, A., Golaz, J.-C., Bodas-Salcedo, A., et al. (2010). Dreary state of precipitation in global models. *Journal of Geophysical Research*, 115, D24211. doi:10.1029/2010JD014532
- Van Leeuwen, P. J., (2010) Nonlinear Data Assimilation in geosciences: an extremely efficient particle filter *QJRMetSoc*, 136, 1991–1996, doi:10.1002/qj.699
- Van Leeuwen, P. J. (2015) Representation errors in Data Assimilation, *Q. J. R. Meteorol. Soc.*, 2014, DOI: 10.1002/qj.2464
- Van Leeuwen, P. J. (2020) A consistent interpretation of the stochastic version of the Ensemble Kalman Filter, *Q. J. Royal Meteorol. Soc.*, doi: 10.1002/qj.3819
- Van Leeuwen, P. J., Y. Cheng, and S. Reich (2015) *Nonlinear Data Assimilation*, Springer, doi:10.1007/978-3-319-18347-3.

Verdoja, F., and V. Kyrki, (2021) Notes on the Behavior of MC Dropout. Presented at ICML Workshop on Uncertainty and Robustness in Deep Learning, Virtual, Online. <https://arxiv.org/pdf/2008.02627.pdf>.

Wang, Z., H. Li, W. Ouyang, and X. Wang (2016) Learnable Histogram: Statistical Context Features for Deep Neural Networks, in B. Leibe et al. (Eds.): ECCV 2016, Part I, LNCS 9905, pp. 246–262, doi: 10.1007/978-3-319-46448-0_15.

Wood, R. (2005). Drizzle in stratiform boundary layer clouds. Part II: Microphysical aspects. *Journal of the Atmospheric Sciences*, 62, 3034–3050.

Wyant, M. C., Bretherton, C. S., Wood, R., Carmichael, G. R., Clarke, A., Fast, J., et al. (2015). Global and regional modeling of clouds and aerosols in the marine boundary layer during VOCALS: The VOCA intercomparison. *Atmospheric Chemistry and Physics*, 15(1), 153–172.

Yu, S., and Ma, J. (2021). Deep learning for geophysics: Current and future trends. *Reviews of Geophysics*, 59, e2021RG000742. doi:10.1029/2021RG000742